

FRESNEL-ZONE MEASUREMENT AND ANALYSIS OF A DUAL-POLARIZED METEOROLOGICAL RADAR ANTENNA

D.B. Hayman, T.S. Bird and G.C. James

CSIRO Telecommunications and Industrial Physics
PO Box 76, Epping NSW 1710, Australia

Abstract

The use of dual polarization in meteorological radars offers significant advantages over single polarization. Recently a standard single-polarization C-band radar was upgraded to operate in dual-polarization mode. The antenna has a 4.2m diameter parabolic reflector with a prime-focus feed. A spherical Fresnel-zone holographic technique was used to obtain the radiation pattern for the upgraded antenna. The sidelobes were higher than predicted and so the data was analyzed to identify the relative contributions of shadowing from the feed crook and surface errors in the dish. This paper describes practical considerations in the measurement of this antenna and the analysis of the results.

Keywords: Antenna measurements, Fresnel zone, Holography.

1. Introduction

There is an increasing use of dual polarization in meteorological radars, particularly for research applications. The additional data provided by dual polarization leads to improved understanding of clouds and precipitation. For instance, droplet size can be estimated using the difference between the vertical and horizontal reflectivities. Larger droplets are more oblate and will have a greater differential reflectivity than smaller droplets [1,2].

The antenna discussed in this paper is based on a standard existing single-polarization-radar system that was upgraded to provide dual polarization capability. The upgrade included a high-power-microwave switch, a dual waveguide run to the antenna and a new feed and orthomode transducer (OMT) for the antenna.

The existing single polarization feed crook was replaced with a dual polarization feed system. An axially symmetric feed with a ring-slot flange was designed, along with an OMT. These were supported by struts and fed by a dual waveguide run. The waveguide was covered with resonant absorber to minimise the effects of reflections. The new feed crook was fitted to the antenna and the antenna measured to check the performance of the upgrade (Fig. 1).

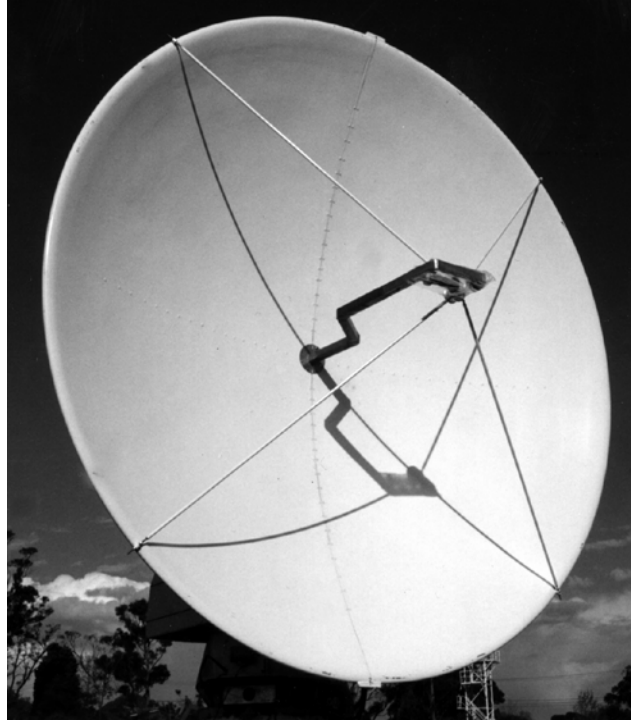


Fig. 1. Antenna with Upgraded Feed.

The target performance for the antenna was specified by the end user and included well matched co-polarized beam patterns, low sidelobes, low cross polarization and high isolation between channels. The basic parameters for the antenna are given in Table 1.

Antenna type	Prime focus fed paraboloid
Diameter (D)	4.2 m
Focal ratio (f/D)	0.34
Half-cone angle	72°
Beamwidth	0.9°
Gain	>45 dBi
Polarization	Horizontal & vertical linear
Frequency	5600 to 5650 MHz

Table 1. Summary of System Specifications.

This paper describes the measurement of the upgraded antenna and an analysis of the results.

2. Antenna Measurement Set-up

The antenna radiation patterns were obtained using a Fresnel-zone holographic technique [3]. All of the measurements were made at the centre frequency, 5.625 GHz. The antenna was too large for our near-field range and we could not measure the far-field directly as our longest range is 40 m and the Rayleigh criterion, $2D^2/\lambda$, is 600 m. For the Fresnel zone approximation to apply, the distance must be more than [3]

$$\frac{\sqrt[3]{D^4/\lambda}}{2} = 9m$$

Our 40 m outdoor range, with its elevation over azimuth rotator, was well suited for this task. Fig. 2 shows a schematic of the measurement set-up and Fig. 3 shows the antenna and source tower. The signal received from the antenna and a reference signal, taken from a coupler placed just before the source horn, were fed into an amplitude and phase microwave receiver. A computer logged the data and drove the antenna in azimuth and elevation to produce a two dimensional map.

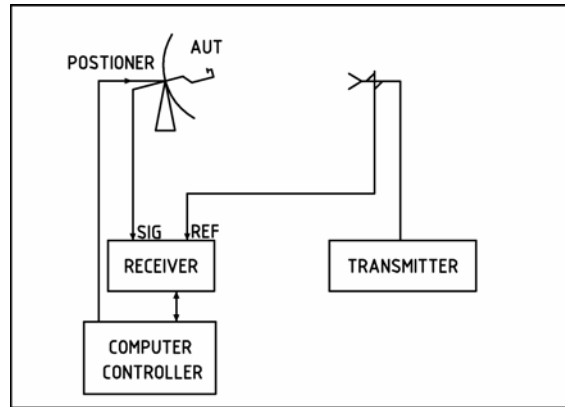


Fig. 2. Measurement Set-up.

The range length of 19 m was chosen as a compromise between the conflicting requirements of minimising ground reflection and interference between the source and antenna under test (AUT).

The radiation pattern was sampled in elevation and azimuth in a rectangular grid over the angular range of -11° to $+10.5^\circ$; the asymmetry was for convenience in processing. This range was chosen to provide sufficient coverage of the sidelobes. The resolution of the aperture field map is given by:

$$\frac{\lambda}{2 \sin \theta}$$

where θ is the half angle of the scan. In this case, the resolution was 5 mm which was adequate for our analysis.



Fig. 3. Outdoor Antenna Range.

The number of samples required is determined by the Nyquist criterion which ensures there is no aliasing of the predicted aperture field. The spacing, in radians, must be no more than the wavelength divided by the diameter of the AUT; for this antenna, converting to degrees, the minimum spacing was 0.73° . We sampled at 0.5° intervals giving a 44×44 point map. Each radiation pattern map took about 50 minutes to complete. The size of the data set for this Fresnel-zone measurement was only about 5% of that required for a near-field measurement giving a considerable saving in measurement time. To compensate for drift in the signal, calibration points were obtained at regular intervals. These were on boresight for the co-polar maps and near a cross-polar peak for the cross-polar maps.

Co- and cross-polarization data were taken with the set-up as described and processed using the following six steps [3]:

- (1) phase and amplitude drifts were corrected by interpolating between the calibration points;
- (2) a correction was made to compensate for the offset in the centre of rotation as the antenna was set above

and forward of the centre of rotation;

(3) the aperture field was calculated by applying a Fourier transform and quadratic phase correction;

(4) a circle with a radius one wavelength larger than the reflector was used as a mask and the field was set to zero outside it to remove measurement artifacts;

(5) a second Fourier transform was applied to produce a two dimensional map of the far-field, covering $\pm 10^\circ$ in both azimuth and elevation;

(6) cardinal and inter-cardinal plane pattern cuts were interpolated from the two dimensional maps.

The results are shown in the following sections.

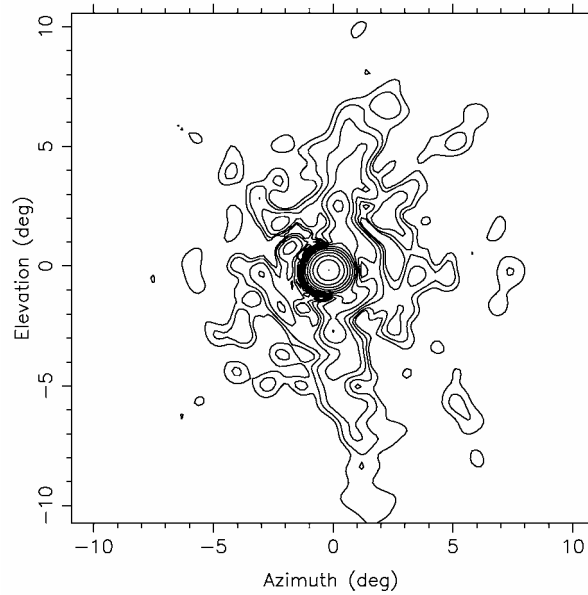


Fig. 4. Measured Co-polar Far-Field Contour Plot with Contours at 3 dB Intervals.

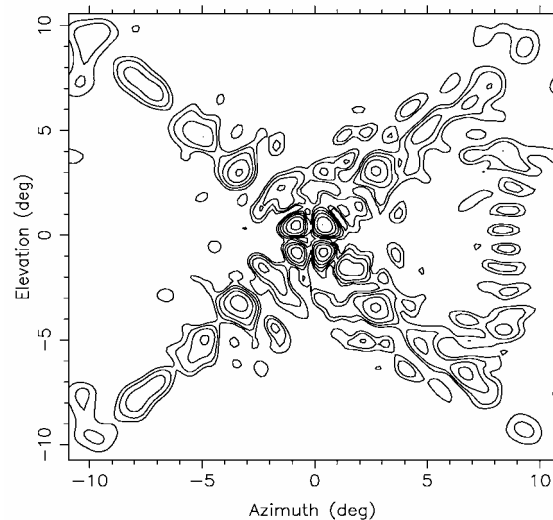


Fig. 5. Measured Cross-polar Far-Field Contour Plot with Contours at 3 dB Intervals.

3. Antenna Patterns

The far-field antenna patterns obtained using the holographic technique are shown in Figs 4 to 8. There was little difference between vertical and horizontal polarization and the results shown are all with the E-

field for the AUT horizontal. The sidelobe mask was supplied as a desired target by the user of the antenna. The aperture amplitude and phase responses were used in analysing the antenna performance (Fig. 9).

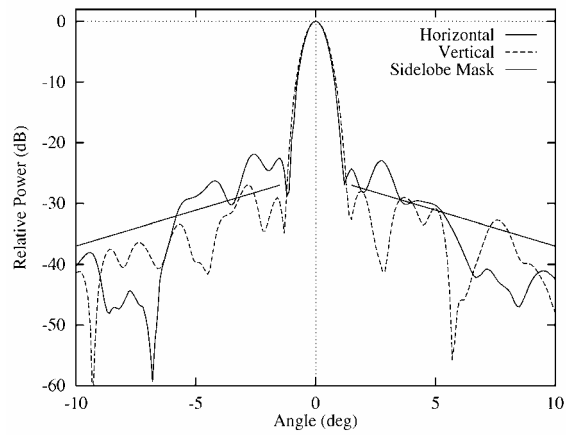


Fig. 6. Measured Co-polar Cardinal Plane Pattern Cuts.

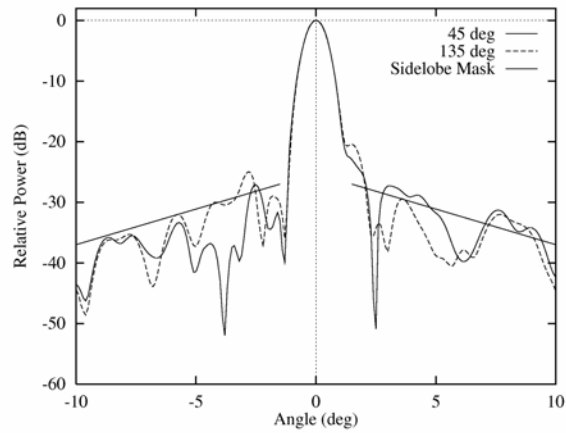


Fig. 7. Measured Co-polar Intercardinal Plane Pattern Cuts.

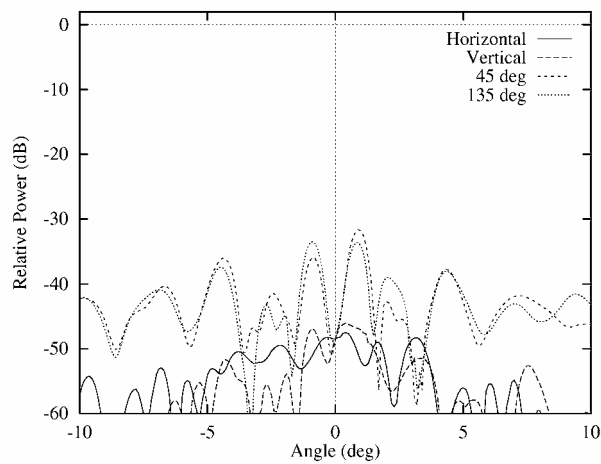


Fig. 8. Measured Cross-polar Pattern Cuts.

Various figures of merit for the antenna were determined from the measurements and most were

satisfactory. The gain, determined through pattern integration, was 45.5 dB. The beamwidth varied from 0.9° to 0.95° . The peak cross-polar level was -32 dB. The patterns from the two polarizations were closely matched. The sidelobes, however, were greater than the desired level, the worst case being -21 dB (Fig. 7).

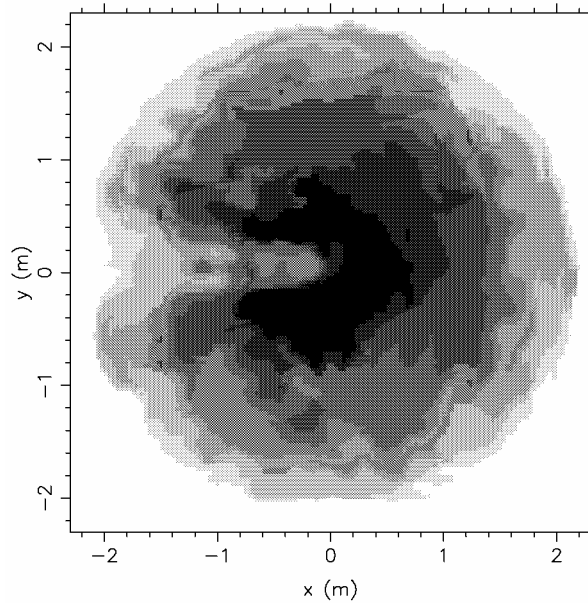


Fig. 9. Measured Aperture Amplitude with a Grey Scale Range of 30 dB.

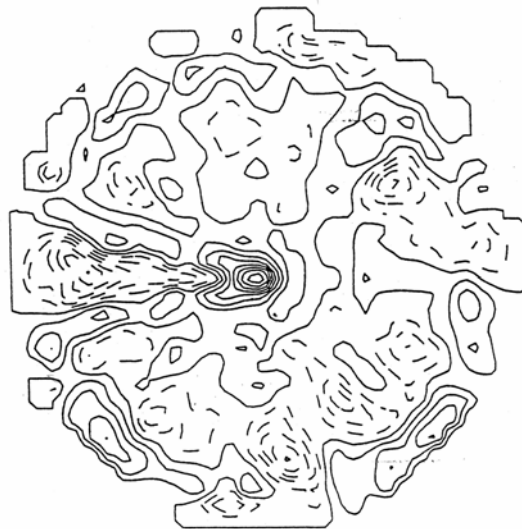


Fig. 10. Surface Errors Normal to Dish Surface with Contours Spaced by 1 mm and Negative Contours Dashed.

4. Sidelobe Analysis

When the antenna was measured, the sidelobe levels were considered too high and some effort went into determining the cause. Preliminary theoretical studies, using a physical optics model, included blockage by the feed but not the feed crook struts. It did not include surface errors in the reflector. The radiation pattern cuts for the model are shown in Fig. 11. The predicted sidelobes are at -32 dB whereas the measurements give sidelobes up to -21 dB.

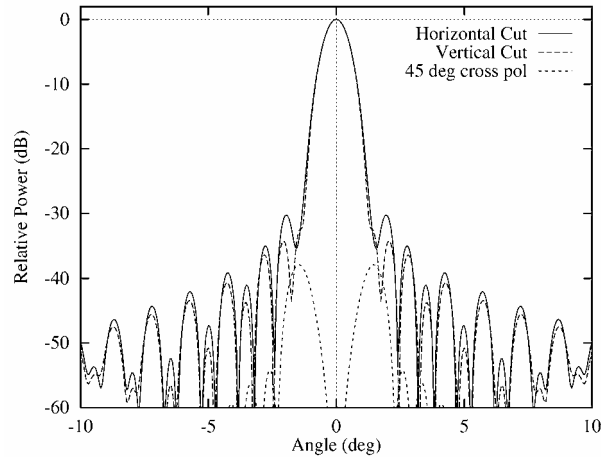


Fig. 11. Preliminary Theoretical Model Cardinal Plane Co-Polarized Pattern Cuts and 45° Cross-Polarized Cut.

Two likely candidates, suggested by the measured aperture data (Figs 9 and 10), for causing the high sidelobes are the feed-crook shadow and the surface errors. The relative effects of these were tested by both manipulating the measured data and modelling them.

The reflector surface errors were calculated by translating the aperture field phase variations into physical deviations normal to the surface of the paraboloid (Fig. 10). The results from the vertically and horizontally polarized measurements were very similar. The assumption that the phase distortions in the aperture were dominated by the surface errors and not scattering from the feed crook or the struts was supported by the random variation and lack of symmetry in the aperture phase. The r.m.s. surface error calculated in this way was 1.6 mm and the maximum deviations were ± 4 mm.

The surface errors were effectively removed from the measured data in the following way. Aperture data was altered by setting all the phase terms to zero; the amplitude data was left unchanged. This approximates the effect of having a perfect dish while retaining the effect of blockage due to the feed and struts present. The effect of the feed-crook and struts on the aperture phase are assumed to be secondary. The aperture field derived in this way was then transformed to give the far-field pattern. The horizontal plane sidelobes dropped from -27 dB to -34 dB, which was below the theoretical level of -32 dB obtained with a perfect paraboloid. The vertical sidelobes fell from -22 dB to -25 dB.

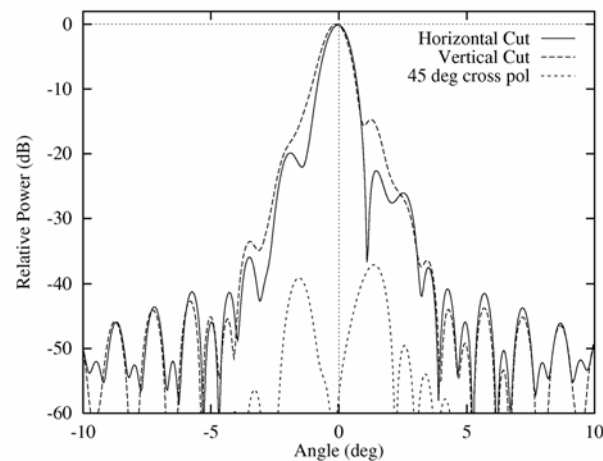


Fig. 12. Theoretical Radiation Pattern Including Surface Errors.

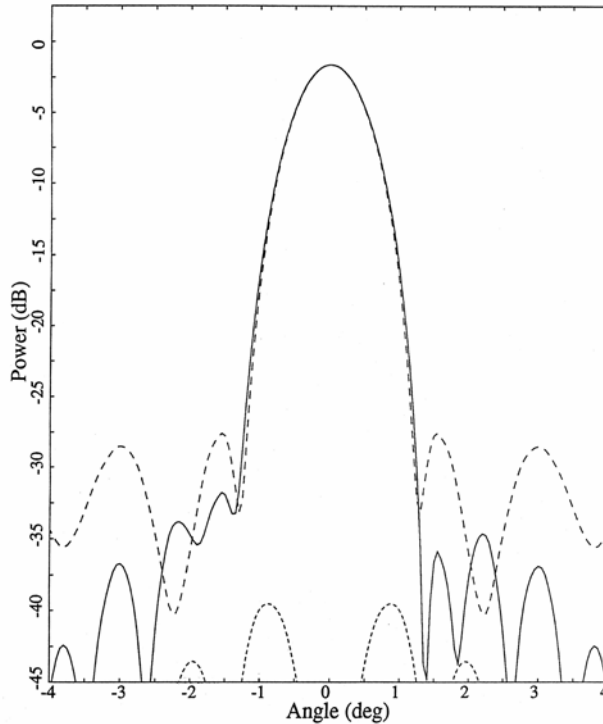


Fig. 13. Theoretical Radiation Pattern Including Feed-Crook Shadow.

The feed-crook shadow was investigated because the amplitude image (Fig. 9) was dominated by it. The struts were not considered because they were not visible in the aperture map. The effect of the shadow was removed from the measured data by filling in the region of the aperture map in shadow (Fig. 9) with values similar to those on either side of the shadow. The feed crook was covered with a resonant absorbing material and so the main effect of the crook was expected to be shadowing. This experiment showed a significant reduction in the vertical plane sidelobes, particularly the second, but made little difference to the horizontal plane.

The surface errors were modelled by introducing the random fluctuations into the surface of the reflector with approximately the same characteristics of those indicated by the aperture map (Fig. 10). The predicted results, shown in Fig. 12, indicate that the surface errors can result in sidelobe levels close to those measured.

The blockage of the feed crook was included in the theoretical model of the antenna by setting the aperture amplitude to zero in a band running from the centre of the antenna to the edge. The width of the band was 150 mm which was similar to that seen on the aperture map derived from measurement (Fig. 9). This model gives sidelobes in the horizontal plane of -35 dB and those in the vertical plane at -27 dB. The level without the blockage was -32 dB (Fig. 13).

Both the theoretical models and manipulation of the measured aperture data give indications of levels of sidelobes but not the precise detail. They do, however, show the same general trends.

It can be concluded that surface errors are the major contributor to the horizontal plane sidelobes. The vertical sidelobes appear to be affected to a similar extent by both the surface errors and aperture blockage.

6. Conclusions

The measurement of an upgraded meteorological radar antenna has been described. The antenna met all the specifications except that the sidelobes were above the desired level. The main causes for this has been shown to be surface errors in the dish and shadowing from the feed crook. To reduce these sidelobes, a superior dish is required and further attention is needed to reduce the effect of blockage by the feed crook.

The manipulation of the aperture fields in both the measured and theoretical data proved an effective tool in

investigating mechanisms affecting the antenna performance.

7. Acknowledgments

The authors thank M. Wright, K. Smart, R. Forsyth, P. Doherty and K. Greene for their assistance with the antenna upgrade and measurements.

References

- [1] D Atlas ed., "Radar in meteorology: Battan Memorial and 40th Anniversary Radar Meteorology Conference", Battan Memorial and 40th Anniversary Radar Meteorology Conference (1987 Boston, Mass.), American Meteorological Society.
- [2] T. Keenan, K. Glasson, F. Cummings, T. Bird, J. Keeler and J. Lutz: "The BMRC/NCAR Polarimetric Radar System", JWA Conference, Tsukuba, Japan. 24-25 Jan 1996.
- [3] G.T. Poulton: "Microwave holography for antenna measurements", IREECON'83, Sydney, Australia, 5-9 September 1983, pp. 256-258.